ELSEVIER

Journal of Alloys and Compounds 452 (2008) 61–66

Journal of ALLOYS AND COMPOUNDS

www.elsevier.com/locate/jallcom

The dependence of the iron–carbon eutectic transition temperature on thermal history and its implications for thermometry

N. Sasajima [a,*], Y. Yamada [a], Y. Wang [a], P. Bloembergen [a], T. Wang [b,1], J. Le Coze [c]

[a] *National Metrology Institute of Japan (NMIJ), AIST, Tsukuba 305-8563, Japan*
[b] *National Institute of Metrology, Beijing 100013, China*
[c] *Ecole Nationale Supérieure des Mines, CNRS-UMR5146, 42023 Saint Etienne, France*

Received 18 September 2006; received in revised form 27 November 2006; accepted 13 December 2006
Available online 16 February 2007

Abstract

The melting behavior of the eutectic Fe–C fixed point was investigated as a function of the thermal history prior to melting using degassed and non-degassed Fe–C cells. The liquidus temperature and the melting range depend on the preceding growth rate: slower freezing entails a higher liquidus temperature and a smaller melting range. Annealing at temperatures just below the eutectic temperature has similar effects. The inflection point of the melting plateau and the maximum temperature of the freezing plateau showed a linear variation with the square root of the growth rate during the (preceding) freeze and this variation is approximately five times smaller for the melt than for the freeze. No clear evidence of the effect of gaseous impurities could be detected on the shape of the melting plateau obtained in conjunction with the lowest growth rate. However, both the inflection point of the melting plateau and the maximum temperature of the freezing plateau showed a larger dependence on the growth rate for the degassed cell.

Keywords: Metal–carbon eutectic; Fixed point; High temperature; Temperature standard; Radiation thermometer

1. Introduction

In thermometry fixed points are used to define the temperature scale and to disseminate the scale to secondary thermometers. Primary fixed points are defined in the International Temperature Scale of 1990 (ITS-90) [1]; the highest temperature of the defining fixed points is that of the copper point (1357.77 K). Above the freezing point of silver (1234.93 K), ITS-90 is defined via extrapolation in terms of the ratio of the spectral radiance of a blackbody with respect to that at either the silver, gold (1337.33 K) or copper freezing point, resulting in a rapid increase of uncertainty of the scale with increasing temperature. To reduce the uncertainty at high temperatures, national metrology institutes are now developing reference fixed points beyond the copper point based upon metal–carbon (M–C) and metal carbide–carbon (MC–C) eutectics covering the range from the 1427 K (Fe–C) up to 3458 K (HfC–C) [2].

To enable the implementation of M(C)–C eutectic systems as practical reference fixed points for use in thermometry, evaluation of their reproducibility is a prerequisite. From previous investigations it appeared that the shape of the melting plateau and its liquidus temperature are significantly affected by the purity of the materials involved [3]. To better understand the influence of impurities on the melting process, melting plateaus of the Fe–C eutectic system, observed for eutectic ingots prepared from iron powder of different purity levels were compared with melting plateaus modeled by means of Thermo-Calc software [4]. The effect of impurities could be quantified but discrepancies between the predictions by the model and the experimental results remained.

As compared to other M–C eutectics, Fe–C showed relatively poor melting plateaus with repeatability in transition temperature of approximately 130 mK [3]. Therefore, in a subsequent investigation, the melting behavior of Fe–C eutectic was measured as a function of the thermal history prior to melting [5]. The results showed that both the liquidus temperature and the

* Corresponding author at: Radiation Thermometry Section, National Metrology Institute of Japan, AIST, Tsukuba Central 3, 1-1-1 Umezono, Tsukuba Ibaraki 305-8563, Japan. Tel.: +81 29 861 4031; fax: +81 29 861 4010.
E-mail address: n.sasajima@aist.go.jp (N. Sasajima).
[1] Guest researcher at NMIJ, AIST.

0925-8388/$ – see front matter © 2007 Elsevier B.V. All rights reserved.
doi:10.1016/j.jallcom.2006.12.158

melting range depend on the growth rate of the solid phase during the preceding freeze: slower freezing entails a higher liquidus temperature and a smaller melting range. Annealing at temperatures just below the eutectic temperature following a fast freeze showed a melting plateau resembling that obtained after a slow freeze.

In the present study, the effect of gaseous impurities on the melting and freezing behavior was investigated experimentally by comparing the results obtained for degassed and non-degassed Fe–C cells because the modeling of their effects on the basis of Thermo-Calc is problematic. This was done by systematically investigating the influence of gaseous impurities on the effect of thermal history of the ingot preceding the melt.

2. Experimental context

2.1. The Fe–C fixed-point cells

For the comparison of degassed (DG) and non-degassed (ND) Fe–C cells, two Fe–C eutectic cells were newly prepared. In a previous investigation [5], the Fe–C cell was constructed from a degassed Fe–C ingot prepared by the high-vacuum cold-crucible induction-heating method. The ingot was cut into strips, and then they were polished, cleaned and filled in the crucible for observation. However, analysis results showed that the levels of both gaseous and metallic impurities were higher than expected, amounting to an overall purity level of about 99.99%. It is suspected that the impurities were introduced during cutting and polishing of the degassed sample.

In the current investigation, to reduce contamination during handling, the high-purity iron was prepared at the Ecole National Superieure des Mines, Saint Etienne (EMSE) in the shape of a cylindrical ingot to fit the shape of the crucible. This moreover results in a reduced contamination with gaseous impurities during handling because of the associated reduced surface area. The ingots were then transferred to the National Metrology Institute of Japan (NMIJ) where they were melted in a graphite crucible to form eutectic Fe–C.

At the EMSE the starting material was electrolytic iron. After melting in a cold-crucible high-frequency induction-heating furnace [6] under high-purity argon to form a compact ingot, this was cut in halves. One piece was kept as the 'non-degassed' sample. The other piece to be degassed was then re-melted under a high-purity mixture of argon and hydrogen for several times and finally under argon to degas hydrogen. Thus, the 'degassed' sample was obtained. Both samples were then hot forged to a diameter close to the inner diameter of the crucible, mechanically cleaned, machined to eliminate possible contamination during hot forging and a central hole was drilled, to accommodate the cavity of the crucible. Machining was performed at a low velocity with liquid cooling. Finally, they were cleaned with organic solvents and then, by acid pickling. A sample was taken from both ingots for impurity analysis.

At the NMIJ, the ingots were placed inside the graphite crucibles, and were melted to form eutectic alloy with carbon, totally supplied from the crucible. The filling was done in vacuum in a vertical furnace (Nagano VR20-A10).

The graphite crucibles were of the same design with an outer diameter of 24 mm and a length of 45 mm. The crucible has a blackbody cavity with an aperture diameter of 3 mm, cavity length of 33.7 mm, and a conical bottom shape with an apex angle of 120°. The wall thickness of the cavity is 2 mm. The effective emissivity of the cavity, taken to be isothermal, was calculated to be 0.9997, assuming diffusely reflecting walls with an emissivity of 0.85. All crucibles with nominal purity of 99.9995% were machined and purified by Toyo Tanso KK.

2.2. Instrumentation

For the investigation of Fe–C eutectic, a three-zone furnace (Chino MAT60SC) [3] was used: temperature uniformity of the furnace was better than 0.1 K over the length of the crucible at the eutectic temperature of Fe–C. The cell was inserted in a graphite cylindrical block which in turn was fitted into a graphite tube, matching the larger size of the furnace tube and placed in the furnace.

The temperature measurements were performed by means of an LP3 radiation thermometer at an operating wavelength of 650 nm. The target diameter is approximately 0.9 mm at a target distance of 700 mm. No correction was applied for the cavity emissivity or the size-of-source effect.

3. Experimental results

3.1. Impurity analysis

Table 1 shows the analysis results in ppm mass for the gaseous impurities for DG and ND ingots. Gaseous impurities were detected by the classical method of infrared absorption after reduction melting (O, N) or after oxidation melting (C, S). Table 2 shows the analysis results in ppm mass for the metallic impurities. Metallic impurities were common to DG and ND ingots, and obtained by glow discharge mass spectroscopy (GD-MS). The total metallic impurities were approximately 21 ppm in mass.

The effect of these impurities on the uncertainty in the Fe–C eutectic system is discussed in detail in [7].

3.2. Melting and freezing plateaus

3.2.1. The effect of gaseous impurities, observed during melting after a slow freeze

After a slow freeze the solidified structure may be assumed to be close to its equilibrium limit, and therefore it is meaningful to firstly have a closer look at this case. Melting and freezing of

Table 1
Detected gaseous impurities in DG and ND ingots (ppm mass)

Ingot	O	C	S	N
DG	3	2	1	1
ND	150	13	1	3

Table 2
Detected metallic impurities in ingots (common to DG and ND) (ppm mass)

Element	Concentration
Al	0.19
Si	0.18
P	0.07
S	0.05
Ti	0.05
Cr	0.94
Mn	0.36
Co	8.7
Ni	0.90
Cu	6.0
Ga	0.02
Ge	2.2
As	0.04
Sr	0.02
Mo	0.30
Ag	0.03
Sn	0.02
W	0.04

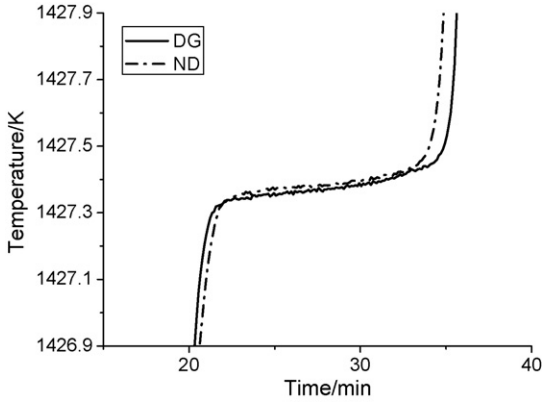

Fig. 1. Melting plateau shape for the degassed (DG) and non-degassed (ND) Fe–C cells obtained after a slow freeze.

the sample are induced by offsetting the furnace temperature T_f with respect to the nominal eutectic transition temperature T_E. The notation $+i$ K or $-j$ K, referred to below, implies melting or freezing plateaus being induced by an offset $T_f - T_E$ of $+i$ K or $-j$ K of the furnace temperature setting, respectively.

The shapes of the melting plateaus observed for the DG and ND samples are shown in Fig. 1. Furnace temperature settings were −1 K for the preceding freeze and +5 K for the melt relative to the eutectic temperature. At the setting of −1 K for the preceding freeze no clear evidence of the effect of gaseous impurities could be detected in the shape of the melting plateau.

3.2.2. *Dependence of the shape of the melting plateau on the rate of the preceding freeze*

Previous investigation showed that the normalized shape of the melting plateau is immune to the melting rate. On the other hand, the melting behavior is influenced markedly by thermal history prior to melting [5]. Therefore, melting plateaus obtained at the same melting rate, i.e. +5 K melts, were compared for various rates $-j$ K of the preceding freeze.

Fig. 2 gives the results for the DG sample. Fig. 2b shows the freezes preceding the melts given in Fig. 2a. The melting plateau was realized after a set length of time (170 min) from the initiation of the preceding freeze, during which time the furnace was kept at the furnace temperature settings to equalize the effect of annealing for all freezing conditions. The melting plateau showed trends similar to those observed in the previous investigation [5]: the higher the rate of the preceding freeze, the lower the liquidus temperature and the larger the melting range, the temperatures traversed during melting.

3.2.3. *Effect of annealing*

The freeze was realized at a −20 K furnace temperature setting and the furnace was then kept at that temperature for annealing during various annealing times, indicated in Fig. 3 for the DG sample. The melt observed after annealing was followed by a −5 K freeze in conjunction with a +5 K melt to check the stability of the radiation thermometer during the annealing experiments.

The large melting range induced by fast freezing (−20 K) is seen to be reduced by annealing. This trend is in good agreement

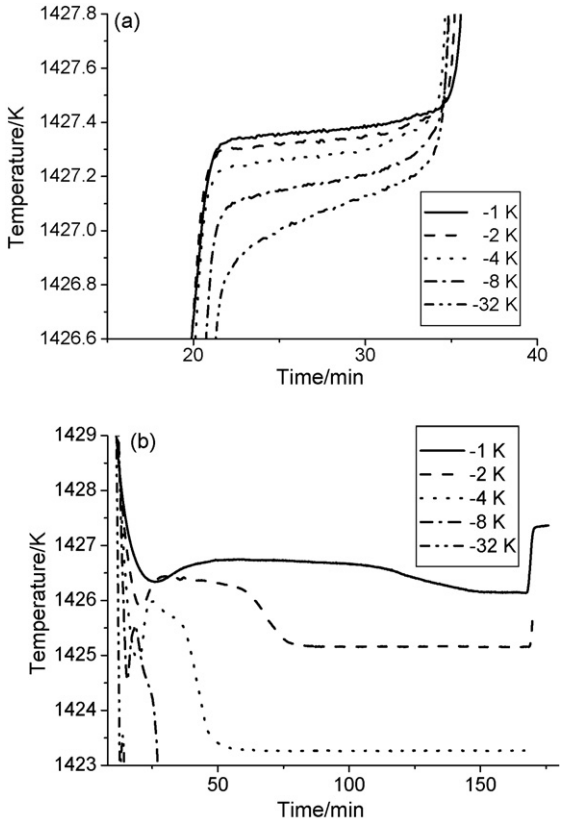

Fig. 2. Degassed (DG) sample: (a) dependence of melting plateaus on the preceding growth rate (determined by the furnace temperature settings, denoted as their difference with respect to T_E) and (b) associated preceding freezing plateaus.

with what has been observed in the previous investigation [5]. From the stability check it appeared that the drift of the radiation thermometer was less than 20 mK during all the measurements, that is, the change in melting temperatures observed in Fig. 3 is significantly larger than the repeatability of the measurement under the same melting conditions.

In the previous investigation, the effect of the annealing temperature was also investigated [5]. From a comparison of the results obtained at annealing temperatures of $T_E - 1$ K and

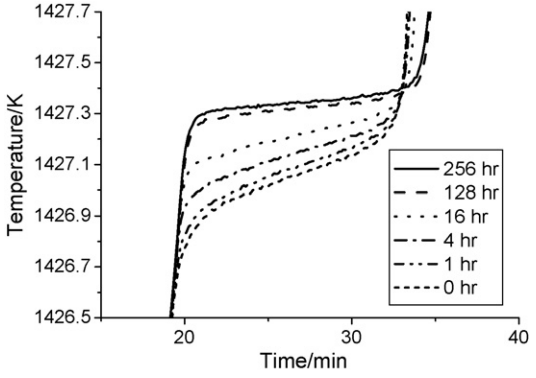

Fig. 3. Degassed (DG) sample: dependence of the melting plateaus on annealing time following a −20 K freeze. Annealing temperature was $T_E - 20$ K.

$T_E - 20$ K after fast freezing (−20 K), it appeared that a higher annealing temperature leads to a shorter annealing time to be required for recovery of the melting plateau to a given shape.

3.3. Microstructures of eutectic Fe–C observed in relation to thermal history

To clarify the origin of the observed phenomena, structural analysis by an optical microscope was conducted for three Fe–C ingots thermally pretreated in a different way [5]. One sample was prepared following a fast freeze (−20 K) and another one following a slow freeze (−4 K). A third sample was prepared following annealing for 128 h at a ($T_E - 20$ K) furnace temperature setting preceded by a fast freeze (−20 K). The samples were rapidly cooled to room temperature, cut into two, polished and etched, and then observed by means of an optical microscope. The result showed that slow freezing results in coarser graphite domains with larger separations within the γ-Fe matrix. Fast freezing resulted in a fine flaky graphite structure. Long-term annealing after fast freezing resulted again in a larger separation of the graphite domains with more rounded shapes. There was no evidence of the formation of Fe_3C (cementite) during the eutectic transition.

From these results, it was concluded that the origin of the dependence of the melting temperature on the rate of the preceding freeze or on the annealing conditions is governed by structural effects, entailing a variation in the overall interfacial free energy when varying these external conditions.

3.4. Relationship between transition temperature and growth rate during freezing

The solidification temperature during directional solidification with imposed growth rate and imposed temperature gradient in the liquid phase is uniquely related to the interlamellar spacing of the eutectic structure via the material parameters characterizing the eutectic system in question. The model [8] predicts that the undercooling, i.e. the temperature difference ΔT between the eutectic temperature – ideally obtained in the limit of zero growth rate – and the solidification temperature observed at finite growth rate is proportional to the square root of the growth rate. This will be further detailed in Section 4.1.

The results obtained for the DG and ND cells were analyzed to see whether the model – in terms of the predicted proportionality – still applies in the present experimental context with imposed rate of heat extraction (rather than growth rate) and a temperature gradient in the liquid state near to zero. The temperature difference ($T_E - T_f$) between the eutectic temperature and the furnace temperature primarily determines the rate of heat extraction. The rate of heat extraction should be proportional to ($T_E - T_f$) if the thermal resistance between furnace and ingot may be supposed to be much larger than that over the transformed part of the ingot, and the variation of the transformation temperature is relatively small. The peak temperatures of the freezing plateaus – with a growth rate uniquely related to the imposed rate of heat extraction – were plotted against the square root of the temperature difference between the eutectic temperature (T_E) and the furnace temperature (T_f) during freezing.

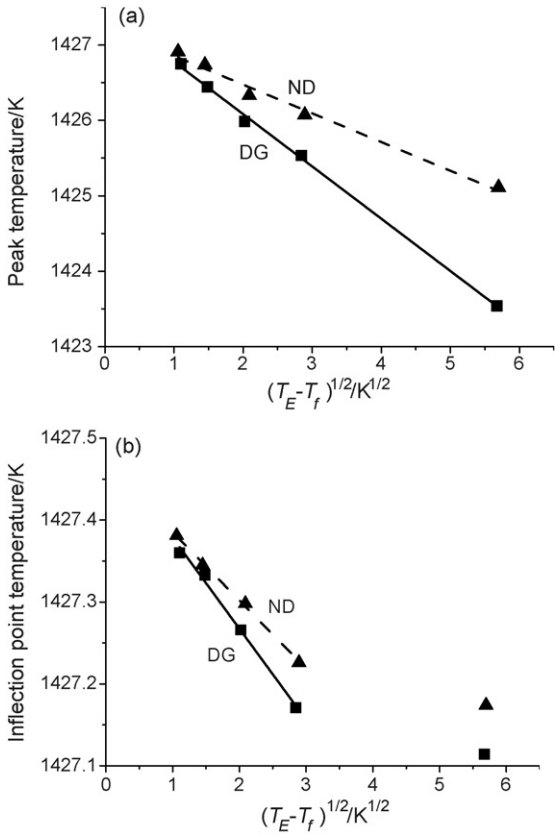

Fig. 4. Degassed (DG) sample vs. non-degassed (ND) sample. Dependence of: (a) the peak temperature of the freezing plateau and (b) the inflection point temperature of the melting plateau on the growth rate during freezing.

The results are shown in Fig. 4a. For the maximum freezing temperature, the plot shows an excellent linear fit for both samples. The slopes of the fits are different, the DG sample showing the larger variation of the undercooling with growth rate.

In Fig. 4b we plot the inflection point temperatures (T_{inf}) of the melting plateaus against the square root of ($T_E - T_f$). Again T_{inf} shows a linear dependence on the square root of the preceding growth rate for both samples[2]; this, to the best our knowledge, is a new experimental finding [9]. The dependence on preceding growth rate for melting is approximately five times smaller than that observed for freezing. The difference observed for the DG and ND samples shows the same trend as in the case of freezing, the DG sample showing the larger slope.

The only difference between the DG and the ND samples is in the amount of gaseous impurities, and therefore it is natural to assume that the difference in the slope is due to this.

[2] Except for the highest growth rate which might be partly explained by the enhanced effect of annealing in the period between freezing and melting, cf. Fig. 2b.

4. Discussion

4.1. Freezing

In the case of alloy solidification, where mass diffusion controls the transformation, atomic movement is required over much larger distances compared to the case of pure substance. Because of these atomic movements, solidification will always require some departure ΔT from equilibrium to drive the process.

For eutectic growth the relationship between the undercooling ΔT, the interphase spacing λ and the growth rate V for a regular eutectic is given in the general form:

$$\Delta T = K_c \lambda V + \frac{K_r}{\lambda} \quad (1)$$

where the coefficients K_c and K_r are related to the material properties [8]. The first term is the so-called solute term, associated with the diffusion of carbon in the liquid phase promoting a fine structure with short diffusion distances between the graphite domains during their growth from the liquid phase. The second term is the so-called solid–liquid interface curvature term promoting a coarse graphite domain structure with low overall interface energy.

Regular eutectics are assumed to grow at minimum undercooling. This leads to the relationships [10]:

$$\Delta T = 2\sqrt{K_c K_r}\sqrt{V} \quad (2)$$

$$\lambda = \frac{\sqrt{K_r/K_c}}{\sqrt{V}} \quad (3)$$

For irregular eutectics like Fe–C (2) and (3) have to be replaced [8], respectively, by:

$$\langle \Delta T \rangle = \left(\phi + \frac{1}{\phi}\right)\sqrt{K_c K_r}\sqrt{V} \quad (4)$$

$$\langle \lambda \rangle = \frac{\phi\sqrt{K_r/K_c}}{\sqrt{V}} \quad (5)$$

Here, the brackets refer to averaged values and ϕ is given by:

$$\phi = \frac{\langle \lambda \rangle}{\lambda_{ex}} \quad (6)$$

where λ_{ex} defines the spacing corresponding to the minimum of the ΔT versus λ curve for a given growth rate V, associated with the results (2) and (3). Although for a given finite temperature gradient in the liquid phase ϕ is a function of V, for eutectic Fe–C in its pure state ϕ is constant up to growth rates from zero to beyond $100\,\mu m\,s^{-1}$ for temperature gradients in the liquid approaching zero [8]. The growth rates corresponding to the furnace temperature offsets ($T_E - T_f$) in Figs. 2 and 4 range from about 1 to $30\,\mu m\,s^{-1}$ calculated from the crucible dimension and the duration of the melting. Since the temperature gradient in the liquid is approaching zero in the limit of zero growth rate in the present experimental context, the relation (4) would imply a square root dependence of the undercooling ΔT on the growth rate V.

4.2. Melting

Apparently the kinetics of melting is not adequately covered by the model proposed in Ref. [8], which is tailored to the description of the process of solidification. For the freeze, the solid–liquid interface is on the average perpendicular to the growth direction. On the other hand melting is initiated at the interface between the graphite and metal-rich phase, showing the highest curvature, resulting in a melting front still more irregular than that developing during freezing. It is therefore surprising that we still see a linear relation similar to the freeze between ΔT and $V^{1/2}$. It is expected that analysis of the eutectic structure will further clarify the relationship between melting temperature and structure: not only the interphase spacing but also interface area and its curvature should be taken into consideration.

4.3. The effect of impurities

The influence of the amount of gaseous impurities on the relation between melting temperature (freezing temperature) and the growth rate during the (preceding) freeze is not yet clear. Apparently nucleation and/or growth of the eutectic phases or diffusion of graphite might be influenced by gaseous impurities, or by their compounds with Fe, C or with some of the metallic impurities, present in the ingot. It even cannot be excluded that the ND samples are purer than the DG samples as regards the metallic impurities due to the 'gettering' effect of the gaseous components. In Ref. [8] a start has been made with quantifying the effect of impurities on the freezing process by studying the variation of the $\Delta T - \lambda$ relationship when varying the material parameters making up the solute and curvature terms K_c and K_r. Further study is needed to estimate the effect of impurities on the material parameters in question such as the interfacial energy incorporated in the interface between the phases involved.

5. Conclusion

The melting behavior of eutectic Fe–C was investigated for two samples, degassed and non-degassed. The melting temperature has been shown to be proportional to the square root of the growth rate during the preceding freeze, as was earlier observed and modeled for the freezing temperature. The observed dependences of the transition temperature on the growth rate have been shown to be influenced by the amount of gaseous impurities, the degassed material showing a larger variation in transition temperature. The variation of the melting temperature with preceding growth rate is approximately five times smaller than that observed for freezing.

Modeling of the observed phenomena in terms of the change in eutectic structure with thermal history is envisaged. It is also envisaged to investigate the effect of gaseous and metallic impurities upon these structural changes.

The saturated melting plateau, resulting from freezing at the lowest growth rate or from annealing at longest annealing time is in reasonably good agreement with the melting plateau modeled on the basis of the Scheil–Gulliver model [5], which takes into account the effect of metallic impurities. The remaining discrepancy is still to be explained.

It should be noted that observation of the relatively small effects of the thermal history on the melting behavior has been enabled only recently through a gradual improvement in measurement capabilities and measurement conditions since the introduction of M–C eutectics as fixed points in thermometry.

The reported thermal influence factors are expected to have minor implications as regards the uncertainty in the definition of the transition temperature of eutectic Fe–C, when standardizing the thermal boundary conditions. M–C eutectics showing higher eutectic temperatures have been shown to be much less prone to thermal history than eutectic Fe–C, the subject of this study [11].

Acknowledgement

The authors would like to thank Professor Wilfried Kurz of the Ecole Polytechnique Federale de Lausanne, Switzerland, for fruitful discussions.

References

[1] H. Preston-Thomas, Metrologia 27 (1990) 3–10.
[2] Y. Yamada, MAPAN-J. Metrol. Soc. India 20 (2005) 183–191.
[3] N. Sasajima, Y. Yamada, B.M. Zailani, K. Fan, A. Ono, Proceedings Tempmeko 2001, VDI Verlag, Berlin, 2002, pp. 501–506.
[4] P. Bloembergen, Y. Yamada, N. Sasajima, S. Torizuka, N. Yoshida, N. Yamamoto, in: D.C. Ripple (Ed.), Temperature: Its Measurement and Control in Science and Industry, vol. 7, AIP, New York, 2003, pp. 261–266.
[5] N. Sasajima, Y. Yamada, P. Bloembergen, Y. Ono, Proceedings Tempmeko 2004, Cavat-Dubrovnik, 2005, pp. 195–202.
[6] J. Le Coze, R. Tardy, A. Kobylanski, M. Biscondi, Proceedings UHPM-94, Japan Institute of Metals, 1995, pp. 371–389.
[7] P. Bloembergen, Y. Yamada, Metrologia 43 (2006) 371–382.
[8] P. Magnin, W. Kurz, Acta Metall. 35 (1987) 1119–1128.
[9] Y. Wang, Internal Report AIST-050126, 2005.
[10] K.A. Jackson, J.D. Hunt, Trans. Am. Inst. Min. Eng. 236 (1966) 1129–1142.
[11] T. Wang, Y. Yamada, Y. Wang, P. Bloembergen, Proceedings SICE Annual Conference 2005, Okayama, 2005, pp. 2739–2743.